FMCW radar for life-sign detection

Laura Anitori, Ardjan de Jong, and Frans Nennie
TNO, Defence, Security and Safety
Oude Waalsdorperweg 63, 2597 AK, The Hague, The Netherlands
Telephone: + 31 70 374 0951
Fax: + 31 70 374 0654
Email: laura.anitori@tno.nl

***Abstract*—In this paper we investigate the use of Frequency Modulated Continuous Wave (FMCW) radars for detecting life-sign of people, i.e. breathing and heartbeat. An optimum frequency has been selected to observe life-sign, taking into consideration also design factors, such as bandwidth availability and interference with other systems. A new compact X-band FMCW radar has been built at TNO laboratories and experimental results are presented here, which demonstrate the ability of this new system to detect life-sign.**

I. Introduction

In the context of the EU-funded SOPRANO Integrated Project a compact FMCW radar has been developed for detecting people breathing and heartbeat frequencies. The goal of the SOPRANO project is to design the next generation of systems for 'ambient assisted living' (AAL) in Europe, to provide a safer and enhanced quality of life by monitoring senior people at home.

By integrating new low-cost technologies and "smart home" systems it is possible nowadays to create a sensor network which can on one hand help older people to live independently in their preferred environment, and on the other hand enables professional outsiders, such as doctors, to monitor their patients living conditions.

In this context the radar can be a useful means to monitor health conditions, specifically breathing and heartbeat rates, of people while they are asleep. While larger motions, such as swinging limbs, can be easily detected with several sensors, e.g. optical or infrared cameras, the detection of breathing and heartbeat is more difficult, due to the small signal amplitudes of the order of a centimeter to a fraction of a millimeter [1]-[3]. For this reason, and because of its ability of contactless and non-cooperative sensing, life sign detection has focused on the use of radar, [4]- [8].

To investigate the practical use of FMCW radar for life-sign detection, we adopted the following approach. First we had to establish which frequency was best suited for measuring life sign signals, as explained in Section II. After the optimal frequency had been selected, a compact X-band radar was built as part of an unobtrusive SOPRANO sensor network that can be installed in a domestic environment. A set of measurements were performed on several people lying in bed, observed from different aspects. These measurements were used to develop and optimize processing techniques for estimation of breathing and heartbeat frequencies. A description of the developed radar, the parameters used to measure life sign, the different processing techniques and the results are given respectively in Sections III, IV and V. From these preliminary results some conclusions are drawn which are reported in Section VI.

II. Selection of carrier frequency

To select an optimum frequency for detecting life sign, we performed a series of radar measurements on six different volunteers, individually lying on a bed in four different positions, namely front view (F) when the radar is illuminating the chest of the person, right (R) and left (L) side view when the radar is illuminating respectively the right and left side, and back view (B) when the radar is illuminating the back of the person, as shown in Figure 1. Four available FMCW radars with carrier frequencies of 2.4 GHz, 5.7 GHz, 9.4 GHz and 24 GHz and linear frequency sweeps (LFS) of respectively 83.5 MHz, 400 MHz, 600 MHz and 250 MHz were used. These bands are in agreement with SRD bands (Short Ranging Devices) according to the Dutch NFP (National Frequency Plan) [9]. The radars were mounted on the ceiling at a distance of about 2.5 m above the persons. The polarization was linear and perpendicular to the long axis of the bed. By comparing all the measurements from the different radars, [10], we conclude that, in most cases, reliable life-sign measurements could be obtained. The similarity of the measurements with the different radar frequencies suggests that the radar scatterers are located on the body surface and the contribution of radiation penetrating inside the body and reflecting on moving parts of heart or lungs is negligible.

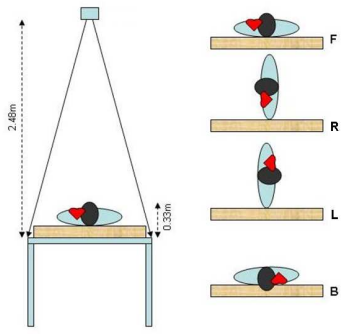

Fig. 1. Set-up showing the four different measurement positions.

978-1-4244-2871-7/09/$25.00 ©2009 IEEE

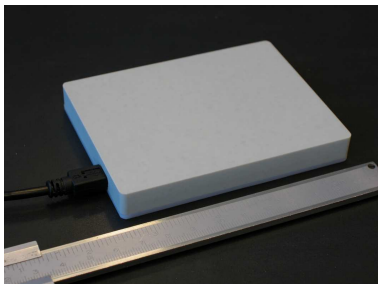

Fig. 2. Compact FMCW X-band radar built by TNO.

TABLE I
X-BAND RADAR SYSTEM PARAMETERS: CARRIER FREQUENCY, PRF, SWEEP RATE, SAMPLING FREQUENCY, RANGE RESOLUTION, MAXIMUM RANGE (WITH ANTI-ALIASING FILTER) AND ANTENNA BEAMWIDTH.

Parameter	Value
P_t	25 mW
F_c	9.6 GHz
PRF	5 KHz
B/T_{up}	800 MHz/80μsec
F_s	3 MHz
δR	18.75 cm
R_{max}	6 m
$\Delta\Omega$	$25^\circ \times 50^\circ$

Since with all frequencies between 2.4 GHz and 24 GHz we were able to see heartbeat and breathing signals in the radar returns, the frequency has been selected on basis of other considerations, such as maximum bandwidth allowed by the local NFP, interference with Wireless LAN (WLAN) and Bluetooth devices, and the undesirability of wall penetration for the given application. As a result of the above considerations, we selected the 9.6 GHz frequency. Moreover, in this band, the technology readiness level is sufficently high for the development of the required components.

III. FMCW X-BAND COMPACT RADAR

A new FMCW X-band radar was built at TNO with the specific aim of keeping it as compact as possible. Compactness of the radar is a prerequisite for the sensor to be deployed in a domestic environment. The dimensions of the complete radar system are $8.2 \times 6.3 \times 1$ cm, as shown in Figure 2.

The transmitting and receiving antennas both consist of 4 patches, and they are designed to illuminate a single bed of standard dimensions from a distance of 2 m. The radar front-end includes an ADC card and the digital beat signal is transferred to a PC via a standard USB connection, which also feeds the source. In Table I the main radar system parameters are given.

Together with the radar system, real-time LabView software was also developed at TNO, which is used for both recording the raw radar data and for real time processing.

IV. LIFE SIGN PARAMETERS

The parameters that we use to describe life sign of sleeping people are heartbeat and breathing frequencies, together with a reliability measure, plus a fifth parameter, that we called life-sign indicator. This indicator is either proportional to the reliability of the estimated respiration frequency or equal to one when the person is moving during his sleep.

If a person is moving while lying in bed, for example when he assumes another position, he is certainly alive, therefore the life-sign indicator is set equal to one. In this last case respiration and heartbeat frequencies can not be measured, because they are too small compared to the body motion and therefore their reliability is set to zero.

Resuming, the five output parameters of the radar system are:

1) f_b: estimated breathing frequency;
2) R_b: reliability measure of the estimated breathing frequency;
3) f_h: estimated heartbeat frequency;
4) R_h: reliability measure of the estimated heartbeat frequency;
5) *LifeSign*: a scalar value giving an overall indication of life sign. This parameter assumes continuous values between 0 and 1, where 1 indicates that the person is moving. In this latest case all the other parameters are set to zero because they are not measurable.

V. SIGNAL PROCESSING AND RESULTS

With the same experimental set-up as described in Section II, a number of measurement were performed to estimate the life sign parameters described in Section IV. During the measurements one of the two radar channels was used for recording the raw radar data while the other one was used to record the signal received from an electrocardiogram (ECG) monitoring device, namely the CS300 Polar Heart Rate Monitor. This device consists of a band which reads the heartbeat rate from the chest and transmits the measured value to the watch. The watch signal is then transmitted to the second radar channel and recorded to verify our results. An optical video camera was also used during the measurements to visually inspect the breathing rate of measured people.

A. Estimation Methods

The recorded raw radar data were processed off line for life sign detection in order to compare different estimation methods for respiration and heart rate. In order to obtain the data in the desired format, some basic pre-processing was performed. The raw radar data consist of time samples, which are arranged in a matrix of size $N_f \times N_s$, where N_f = fast time samples in up sweep and N_s = slow time samples. Since the PRF is very high for our application, we performed a decimation of the slow time samples by a factor of 50, thus the decimated PRF is $\text{PRF}_d = 100$ Hz. The decimation is performed using an overlapping factor of 50% and by applying a Hanning window to each data block. Then an FFT is performed along the fast time axis for range compression, and we obtain the desired range-slow time matrix. Given the geometry of the problem (extended target, range bin size and antenna beamwidth) and the fact that we know the distance radar-target, we can estimate that a person typically extends

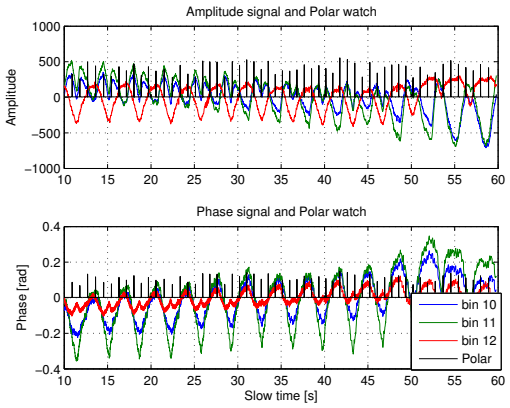

Fig. 3. Breathing amplitude and phase signals of a person measured in left view (L) for 60 seconds for 3 neighboring range bins. The heartbeat rate measured with the Polar watch is plotted in black.

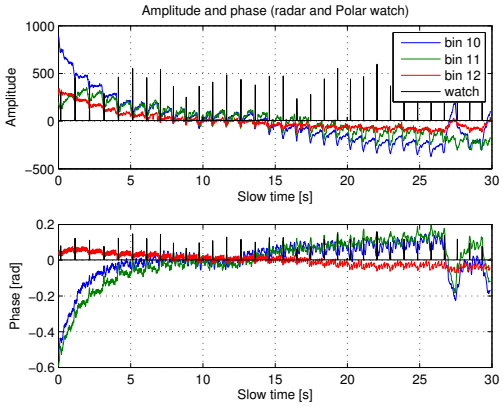

Fig. 4. Heartbeat amplitude and phase signals of a person measured in left view (L) for 60 seconds for 3 neighboring range bins. The heartbeat rate measured with the Polar watch is plotted in black.

over 2 to 3 range bins of about 18 cm size and therefore we can focus on the time signals received from these few neighboring range bins. The selected range bins will be used for estimation of the 5 life sign parameters described in Section IV. Both amplitude and phase of the complex time signal contain information about the target movement inside the range bin. Specifically the upper body part is the dominant movement for breathing, with a displacement of the order of a few millimeters to a few centimeters, depending on the person, while arteries all over the body, pulsing with same rate as the hearth, generate a displacement of the order of 0.1 to 1 mm which can be used for heartbeat measurement. Although the two signals are superimposed on each other in the time domain, they belong to different frequency bands and can be separated in the frequency domain. For people at rest in general the heart rate varies between 0.8 and 1.5 Hz, while the breathing rate varies between 0.1 and 0.4 Hz.

An example of the measured heartbeat and respiration signals (amplitude and phase) is shown in Figures 3 and 4, for a 50 year old man who is lying in bed on his right side (L). In total 6 different people of different ages were measured with the radar and the Polar watch in four different positions. In one measurement series people were asked to breath normally and the data were recorded for 60 seconds. In another measurement series, people were asked to hold their breath for 30 seconds. This second series was used to measure the heartbeat signal alone (as in Figure 4) and compare it with both the heartbeat signal extracted from a normally breathing person and the ECG device.

In Figure 3 a periodicity of about 4 seconds can be seen in both the amplitude and phase signals, which is in agreement with the average breathing rate of an adult person. Likewise, in Figure 4 a periodic signal of about 0.9 seconds can be observed, which falls within the range of adult heartbeat rates of 60 to 100 beats per minute. It is important to notice that for certain bins the amplitude of the breathing signal shows two maxima per breathing period, as in bins 10 and 11 of Figure 3. This happens when the target oscillates through the center of a range bin. However, this phenomenon could also be due to different body parts moving inside a single range bin.

Due to the distinct periodicity of the signals an automatic procedure to extract breathing and heartbeat frequencies can be applied. Nevertheless, as it will be shown later, the separation of the two signals is not so straightforward, mainly do to the fact that, although periodic, the dominating breathing signal is not a perfect periodic sinusoidal wave. On the one hand, when the respiration signal is highly periodic during the integration time (but still not sinusoidal) harmonics of higher order are quite strong and some fall into the frequency band of the heartbeat signal. On the other hand when the breathing signal is not periodic the whole spectrum is full with frequency components which could be high enough to mask the heartbeat frequency.

For this reason two different methods have been used for estimating respiration and heart rates and a comparison is reported below. The estimated rates are updated every 5 seconds and the integration time should contain at least two periods of the breathing or heartbeat signal. Thus, since heart rate must be extracted from the respiration signal, a minimum integration time of 15 seconds is required. Given that a longer integration time provides a better resolution, but a shorter one can better estimate the rate changes, different integration times of 15, 20 and 30 seconds are used and compared.

B. Method 1-FFT

A first approach for estimation of the two frequencies is to apply an FFT. Since the respiration and heartbeat signals have different frequencies it is not necessary to apply a low or high pass filtering. In order to reduce the sidelobes, a Hanning window is applied to the time signal before FFT. We will consider the amplitude and phase signals separately and we will compare the results obtained by applying the same method to both of them. In Figure 5 the spectrum of the amplitude and phase signals of Figure 3 are shown for an integration time of 30 seconds (namely the first 30 seconds).

It is clear from Figure 5 that the respiration rate is easily detectable by simply taking the frequency corresponding to the maximum peak in the breathing frequency window. For all the measurements performed (different people and different positions) the spectrum in this region looks similar, thus making the respiration rate estimation relatively easy. As a measure for the reliability of the estimated frequency we take 1 minus the square root of the Noise-to-Signal Ratio calculated in the frequency region of interest. The reliability is calculated for all the three bins and the estimated breathing frequency is taken from the bin with maximum R_b.

Unfortunately for the heartbeat frequency the rate estimation is not as simple. In fact in the frequency band between 0.8 and 1.5 Hz, where we look for heartbeat frequency, several other frequency components due to the breathing signal are visible, and in some cases the harmonic components of the breathing signal have significantly higher amplitude than the heartbeat component itself. In principle we could think of excluding the peaks at frequencies multiple of the fundamental breathing frequency, but then we would risk to also remove the heartbeat frequency since they may overlap. This is indeed the case for the signal shown in Figure 5. The behavior of these signals is of course different from measurement to measurement and cannot be generalized, thus making it difficult to select the heartbeat rate.

Nevertheless, for some "well-behaved" bins the peak corresponding to the heartbeat signal is higher than the respiration signal harmonics, thus we could estimate f_h using the spectrum of that single bin, as it happens for example in the amplitude signal spectrum of bin 12 or in the phase signal spectrum of bin 10 and 11 in Figure 3. Thus, in this particular case, for estimating correctly f_h we would have to select bin 12 if we would use the FFT of the amplitude signal and bin 10 or 11 if we would use the FFT of the phase signal.

To determine which one is the best bin for estimating f_h, we tried and compared three different methods:

1) select the signal of the bin for which R_b was maximum;
2) select the signal of the bin with the highest amplitude of the breathing peak;
3) select the signal of the bin with minimum fifth order harmonic distortion HD_5, where

$$HD_5 = \sqrt{\sum_{n=2}^{n=5} \left(\frac{A_{n_{f_b}}}{A_{f_b}} \right)^2} \qquad (1)$$

and $A_{n_{f_b}}$ is the spectrum amplitude corresponding to the n-th harmonic of the estimated f_b.

An overview of the different methods performance for heart rate estimation for different integration times is reported in Section V-D.

To show that indeed we are able with this radar to measure also the heartbeat signal, we report in Figure 6 the spectrum of the signal in Figure 4. In this case, for which the measured person was holding his breath, we measured the heartbeat signal alone and the peak in the radar signal spectrum is exactly matching with the ECG spectrum peak. Although the DC component was subtracted from the radar signals before taking the FFT, a low frequency component is still visible in the radar signal spectra and this is caused by a drift of the signal amplitude during the integration time.

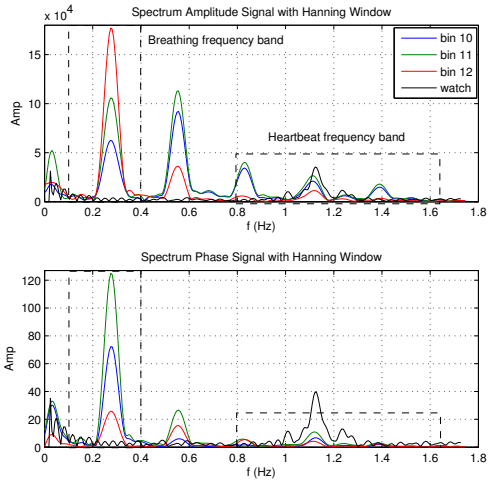

Fig. 5. Spectrum of amplitude and phase signals with Hanning window. The three range bins of interest are shown in different colors for the same measurement as in Figure 3. The amplitude spectrum of the Polar watch signal is also plotted in black. The Polar watch amplitude spectrum has been multiplied by a constant scaling factor to match the figure axis.

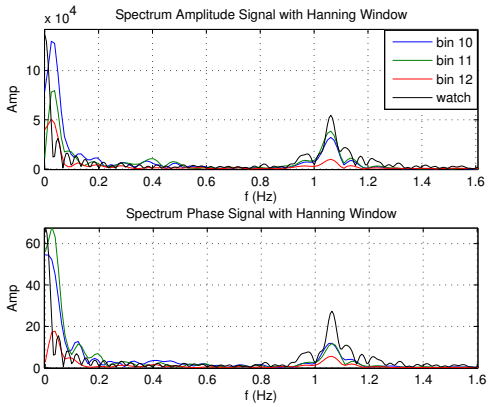

Fig. 6. Heartbeat amplitude and phase signals spectrum with Hanning window. The three range bins of interest are shown in different colors for the same measurement as in Figure 4. The amplitude spectrum of the Polar watch signal is also plotted in black. The Polar watch amplitude spectrum has been multiplied by a constant scaling factor to match the figure axis.

C. Method 2-Autocorrelation

The autocorrelation function is often used for estimating the periodicity of a signal. For a periodic, time limited signal, the autocorrelation function goes to zero and has peaks corresponding in time to multiples of the basic period. For a length N signal $x(n)$, the autocorrelation function is defined

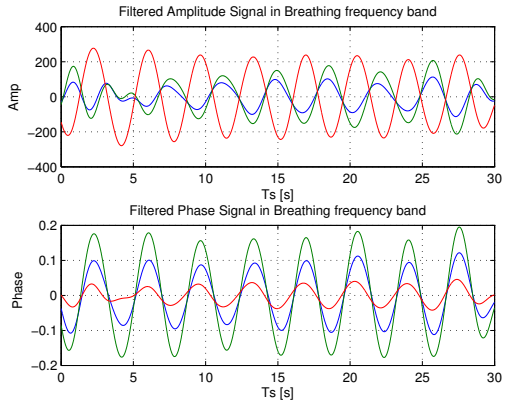

Fig. 7. Amplitude and phase signals after band pass filtering in the breathing frequency region. The three range bins of interest are shown in different colors for the same measurement as in Figure 3.

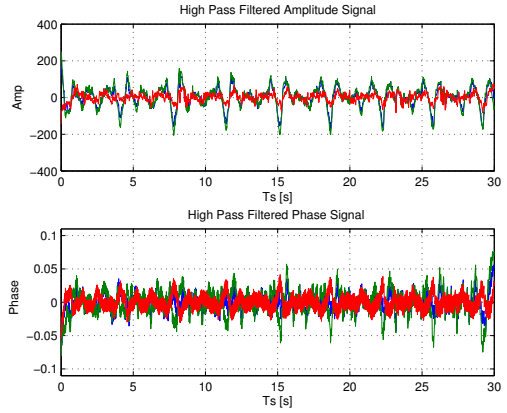

Fig. 8. Amplitude and phase signals after band pass filtering in the heartbeat frequency region. The three range bins of interest are shown in different colors for the same measurement as in Figure 3.

as

$$R_{xx}(m) = K \sum_{n=-N}^{n=N} x(n+m)x^*(n) \qquad (2)$$

where K is a normalization factor, * denotes complex conjugate and m is the lag at which the autocorrelation function is evaluated. To estimate the respiration and heartbeat time period, we apply in the frequency domain an ideal band pass filter with cut-off frequencies 0.05 Hz and 0.5 Hz to the breathing signal spectrum. After the filtering we go back to the time domain and the autocorrelation function of the resulting signal is evaluated. The respiration period is then estimated to be the time corresponding to the autocorrelation peak in the time interval between 0.6 and 1.33 seconds, the inverse of which provides the breathing rate.

For heartbeat rate we apply to the original breathing signal an ideal high pass filter with cut-off frequency 0.8 Hz and then we calculate the autocorrelation of the filtered time signal and look for the peak in the time interval where we expect to find

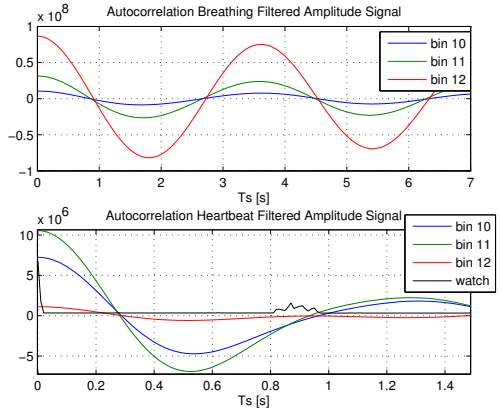

Fig. 9. Autocorrelation of the amplitude signal after band pass filtering in the breathing frequency region (top) and in the heartbeat frequency region (bottom). The three range bins of interest are shown in different colors for the same measurement as in Figure 3. For the heartbeat filtered signal also the autocorrelation of the Polar watch is plotted in black as ground truth. The Polar watch autocorrelation function has been multiplied by a constant scaling factor to match the figure axis.

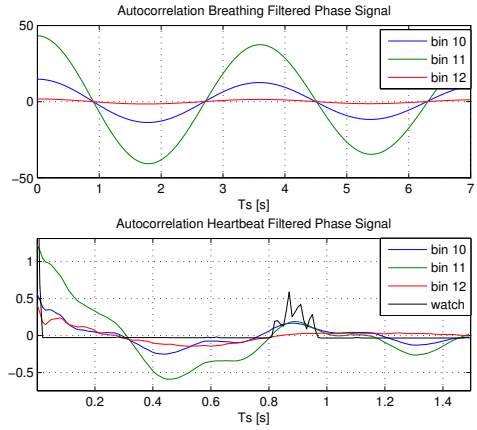

Fig. 10. Autocorrelation of the phase signal after band pass filtering in the breathing frequency region (top) and in the heartbeat frequency region (bottom). The three range bins of interest are shown in different colors for the same measurement as in Figure 3. For the heartbeat filtered signal also the autocorrelation of the Polar watch is plotted in black as ground truth. The Polar watch autocorrelation function has been multiplied by a constant scaling factor to match the figure axis.

the heartbeat. In Figures 7 to 10 the filtered time signals and the respective autocorrelation functions are shown for both amplitude and phase.

For the reliability of the estimated periods we use a measure of the signal periodicity. In fact for a time limited, perfectly periodic signal, the amplitude of the peak occurring at the first basic period of the signal would be $A_2 = E(1 - \frac{1}{N})$, where E is the signal energy, corresponding to $R_{xx}(0)$, and N is the number of periods in the integration time. Therefore we measure R_b and R_h as

TABLE II
PERFORMANCE OF THE DIFFERENT PROCESSING TECHNIQUES (FFTS WITH METHODS 1, 2 AND 3 AND AUTOCORRELATION FUNCTION OF AMPLITUDE AND PHASE SIGNALS) FOR ESTIMATION OF f_h WITH DIFFERENT INTEGRATION TIMES.

	15 secs	**20 secs**	**30 secs**
FFT Amp, 1	38.6%	45.5%	48.7%
FFT Amp, 2	39.5%	40.4%	44.2%
FFT Amp, 3	42.7%	45.5%	49.4%
FFT Phase, 1	45.9%	51.5%	55.2%
FFT Phase, 2	32.3%	34.9%	38.3%
FFT Phase, 3	49.1%	50.5%	55.2%
AC Amp	27.7%	26.3%	24.7%
AC Phase	25%	26.7%	22.7%

$$R = \frac{\frac{\hat{A_2}}{E}}{1 - \frac{1}{\hat{N}}} \tag{3}$$

where the denominator of equation (3) is the theoretical value of the ratio A_2/E if the signal would have exactly $\hat{N}$ periods in the integration time, where $\hat{N}$ is the ratio between the integration time and the estimated signal period.

As can be seen from Figures 9 and 10, breathing rate can be estimated quite accurately with both phase and amplitude signals. For the case shown in these two figures, the heart rate could also be successfully estimated by using bin 12 for Figure 9, and bin 10 or 11 for Figure 10.

D. Methods Comparison

A comparison of the results obtained for estimation of f_h with the different methods is reported in Table II. For all the techniques used and for all the integration times, a percentage value is calculated as the ratio between the number of times that f_h was successfully estimated within an error of $\pm 5\%$ from the ECG measured rate and the total number of data blocks used (which varies depending on the integration time). In total we used 24 of the 30 available measurements for the calculations in Table II, since 6 of them had to be discarded. The percentage show that for this set of measurements the best method for estimation of heart rate was the phase FFT method with about 55% correct estimations. If an error of $\pm 10\%$ is allowed, then the correct estimations increase to about 60%. Anyway a definitive conclusion can not be drawn on the algorithm to be used since many more measurements would be required to obtain reliable statistics. What can be seen from Table II is that, at least for the FFT methods, a longer integration time is preferable. Comparison results are not reported for estimation of f_b, since all the methods are equally good and therefore the processing technique should be selected on the base of best heart rate estimation.

VI. CONCLUSION AND FUTURE WORK

In this paper we present results of a series of measurements of people breathing and heartbeat signals performed with an X-band FMCW radar. The results show that respiration rate can be accurately extracted using conventional signal processing techniques. The heartbeat signal is also clearly visible when measured alone but it is more difficult to estimate heart rate in presence of the breathing signal. In the future more measurements should be made to determine which one of the analyzed methods is best and more signal processing techniques should be investigated for tackling this problem. Less conventional techniques, such as non linear processing and principal components analysis will be used in the future to compare the results with the current ones.

Nevertheless, for the purpose of establishing if a person is still alive while sleeping, the breathing rate measured with the current FMCW radar proves to give satisfactory results. In fact breathing frequency was always successfully estimated for all different people in all different positions.

ACKNOWLEDGMENT

The work presented in this paper has been funded by the European Commission within the SOPRANO (Service-oriented Programmable Smart Environments for Older Europeans) Integrated Project under Framework Programme 6 (FP6). More information are available at http://www.soprano-ip.org.

The authors would like to thank Noud Maas, Roland Bolt, Henjo Schot and Christiaan Lievers for their work and support on hardware and software.

REFERENCES

[1] A. Periasamy, and M. Singh, "Reconstruction of Cardiac Displacement Patterns on the Chest Wall by Laser Speckle Interferometry", *IEEE Transactions on Medical Imaging*, vol. 4, no. 1, pp. 52-57, March 1985.

[2] G. Ramachandran, and M. Singh, "Three-Dimensional reconstruction of Cardiac Displacement Patterns on the Chest Wall during the P, QRS and T-segmants of the ECG by Laser Speckle Interferometry", *Medical and Biological Engineering and Computing*, vol. 27, pp. 525-530, 1989.

[3] T. Kondo, T. Uhlig, P. Pemberton, and P. D. Sly, "Laser Monitoring of Chest Wall Displacement", *European Respiration Journal*, vol. 10, no. 8, pp. 1865-1869, 1997.

[4] I. Y. Moskalenko, "Application of Centrimetre Radio Waves for Non-contact Recording of Changes in Volume of Biological Specimens", *Biophysics*, vol. 5, no. 2, pp. 225-228, 1960.

[5] C. C. Johnson, and A. W. Guy, "Nonionizing Electromagnetic Wave Effects in Biological Materials and Systems", *Proceedings of the IEEE*, vol. 60, no. 6, pp. 692-718, June 1972.

[6] C. I. Franks, B. H. Brown, and D. M. Johnston, "Contactless Respiration Monitoring of Infants", *Medical and Biological Engineering*, vol. 14, no.3, pp. 306-312, May 1976.

[7] C. I. Franks, J. B. G. Watson, B. H. Brown, and E. F. Foster, "Respiratory Patterns and Risk of Sudden unexpected death in Infancy", *Archives of Disease in Childhood*, vol. 55, pp. 595-599, 1980.

[8] J. C. Nelson, J. C. Lin, and M. E. Ekstrom, "Teratological Studies of Fetal Exposure of Mice to RF Radiation", *Microwave Symposium Digest, MTT-S International* vol 79, no. 1, pp. 45-46, April 1979.

[9] Agentschap Telecom, Nationaal Frequentieplan, 2005.

[10] A.J. De Jong, and L. Anitori, "Life-sign detection with FMCW radar", *NATO symposium*, Mannheim, Germany, April 2008.